Structural Engineering and Mechanics, *Vol. 63, No. 6 (2017) 725-734*
DOI: https://doi.org/10.12989/sem.2017.63.6.725

Bond deterioration of corroded steel in two different concrete mixes

Haijun Zhou*, Xuebing Liang[a], Zeqiang Wang[b], Xiaolin Zhang[c] and Feng Xing[d]

Guangdong Provincial Key Laboratory of Durability for Marine Civil Engineering, Shenzhen University, China

(Received October 28, 2016, Revised April 12, 2017, Accepted May 1, 2017)

Abstract. This paper investigated the effects of rebar corrosion on bond performance between rebar and two different concrete mixes (compressive strengths of 20.7 MPa and 44.4 MPa). The specimen was designed as a rebar centrally embedded in a 200 mm concrete cube, with two stirrups around the rebar to supply confinement. An electrochemical accelerated corrosion technique was applied to corrode the rebar. 120 specimens of two different concrete mixes with various reinforcing steel corrosion levels were manufactured. The corrosion crack opening width and length were recorded in detail during and after the corrosion process. Three different loading schemes: monotonic pull-out load, 10 cycles of constant slip loading followed by pull-out and varied slip loading followed by pull-out, were carried out on the specimens. The effects of rebar corrosion with two different concrete mixes on corrosion crack opening, bond strength and corresponding slip value, initial slope of bond-slip curve, residual bond stress, mechanical interaction stress, and energy dissipation, were discussed in detail. The mean value and coefficient of variation of these parameters were also derived. It was found that the coefficient of variation of the parameters of the corroded specimens was larger than those with intact rebar. There is also obvious difference in the two different concrete mixes for the effects of rebar corrosion on bond-slip parameters.

Keywords: reinforcement; concrete; corrosion; bond; cyclic-loading; performance degradation

1. Introduction

Reinforced concrete infrastructures are vulnerable to environmental corrosion, which raises durability issues as relates to long-term load-carrying performance. Corrosion of reinforcement normally occurs due to attack by aggressive agents such as chloride ions from the marine environment. Also, rebar corrosion induces the following consequences: cross section area reduction of rebar, possible cracking of the concrete cover, and deterioration of bond between rebar and concrete. Bonding is essential for the composite action of reinforced concrete structures as it facilitates load transfer across the steel-concrete interface. There have been many investigations in the literatures about bonding behaviors between rebar and concrete by means of experimental and analytical studies. Eligehausen *et al.* (1983) investigated the bond performance by monotonic and cyclic loading tests and formulated models according to the experimental results. It is now well understood that bonding behaviors primarily depend on three factors: the compressive strength of concrete, confinement, and the surface of the steel (deformed or round) (Wu and Zhao 2013). Serhat and Metin (2015) further investigated bond-slip modeling methods used in FE analysis of RC members and found that bond-slip modeling is more suitable with spring elements.

Corrosion of steel will produce rust with volume expansion and change the interface between steel and concrete, thus inevitably changing the bonding behaviors. Almusallan *et al.* (1996) evaluated the effects of corrosion on the bond strength. Mangat *et al.* (1999) studied bond characteristics of corroding steel in concrete beams and the results confirmed the effects of corrosion on anchorage length. Fang *et al.* (2004) investigated the corrosion effects on bond in reinforced concrete by monotonic pull-out loading; Fang *et al.* (2006) further studied effects of corrosion by way of cyclic loading tests. Bhargava *et al.* (2008) suggested empirical models for corrosion-induced bond degradation in reinforced concrete. Zhao *et al.* (2013) studied bond behavior of normal/recycled concrete with corroded steel bars. Akshatha *et al.* (2014) investigated flexural bond strength behavior in Ordinary Portland Cement concrete of National Bureau of Standard beams for various corrosion levels, the results showing that the bond strength decreased as the amount of corrosion increasing. Kivell *et al.* (2015) investigated the bond performance under monotonic and cyclic loading and formulated a model based on the test results. Chen *et al.* (2015) presented a time-dependent reliability analysis of corrosion affected RC structures and the associated bond strength degradation, and found that the proposed approach is capable of assessing performance of the bond strength of concrete structures affected by reinforcement corrosion during their life cycle. Although there are some results in the literature on the

*Corresponding author, Ph.D.
E-mail: haijun@szu.edu.cn
[a]Postgraduate
E-mail: 1308437613@qq.com
[b]Undergradua
E-mail: 1043912197@qq.com
[c]Postgraduate
E-mail: 1432301813@qq.com
[d]Professor
E-mail: xingf@szu.edu.cn

ISSN: 1225-4568 (Print), 1598-6217 (Online)

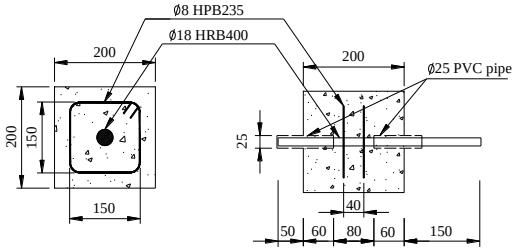

Fig. 1 Specimen geometry (Unit: mm)

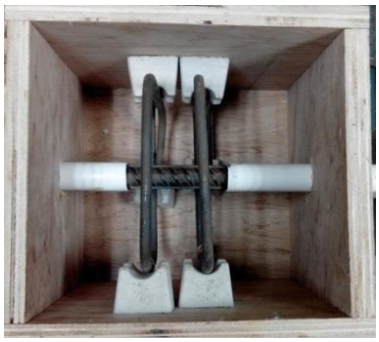

Fig. 2 Mould and reinforcement

effects of corrosion on bond performance, there are still many unsolved issues due to the complexity of the interface problem together with the random nature of corrosion. Sæther (2009) collected ten tests results, and the data showed significant variations. The reasons might be due to the randomness of corrosion itself, or difference in experimental setup, dimensions of specimens, and the use of concrete mixes with different concrete strengths. A recent test by Yalciner *et al.* (2012) shows that the higher the concrete strength, the higher the percentage of bond strength degradation due to steel corrosion; and this point still needs further investigation and verification.

In this paper, originated from the above issues, an experimental study on bond behavior of corroded rebar was carried out with two different concrete mixes. The parameters related to bond-slip curves were derived by three different loading schemes. The coefficient of variation of each parameter was derived to account for the random nature of corrosion. The test, together with previous studies about the effects of stirrup corrosion alone on bond-slip performance with transverse reinforcement (Zhou *et al.* 2015a), could further clarify the effects of reinforcement corrosion on bond-slip behaviors.

2. Test setup and procedure

2.1 Test specimens

The configuration of test specimens followed the previous tests (Zhou *et al.* 2015a). Fig. 1 shows ϕ18 mm deformed rebar with two confinement stirrups (ϕ8 mm) set in a concrete prism. 2 PVC pipes were used to limit the bond length of rebar to 80 mm. The bond stress along the rebar was considered to be uniform in view of the fact that the bond length was much less than the development length of the rebar. The two closely-spaced stirrups provided lateral restraint along the bond length and helped to limit any effects of the end (Fig. 2). There were 120 specimens cast in total in this test: 60 specimens with concrete design strength of 20 MPa, and the other 60 specimens with concrete design strength of 40 MPa.

2.2 Material properties

There were two different kinds of concrete mixes, and the strength grades of concrete being C20 and C40. The first kind of concrete mix proportion was Portland-cement:water:sand:stone=1: 0.6 : 2.24 : 3.68. The other mix proportion was Portland-cement:water:sand:stone=1:0.48: 1.62:2.88. Moreover, nine concrete cubes with dimensions of 100mm×100mm×100 mm were also cast for compressive strength testing for each concrete mix. The two concrete mixes were found to have 28-day average compressive strengths of 20.7MPa and 44.4MPa, respectively.

2.3 Accelerated corrosion program

An electrochemical accelerated corrosion technique was used to corrode the specimens. This technique involved conducting a direct current through the specimens to accelerate the oxidation process of rebar in a 5% NaCl solution (Fang *et al.* 2006). The average corrosion level was estimated according to the target mass loss of the rebar to setup different corrosion levels for the rebar. The theoretically calculated mass loss, in terms of the electrolytic time, can be expressed by Faraday's Law

$$T = \frac{m_t \times 2 \times F}{I \times 55.847} \quad (1)$$

where T is the corrosion duration time, m_t is the mass loss, I is the average electrical current and F is the Faraday constant. The stirrup was not corroded in this test.

The current density of this experiment was set as 300 μA/cm^2, and a 13.57 mA constant corrosion current was applied to each corroded specimen. The current density of 500 μA/cm^2 was the maximum for electrochemical accelerated corrosion in concrete (Coronelli *et al.* 2013). The accelerated corrosion of the rebar was actually carried out in 3 specimens as one group (Fig. 3). The experimental research program consisted of testing a total of 120 reinforced concrete specimens with five different corrosion levels of 0%, 5%, 10%, 15% and 20%. The maximum time was 92 days to achieve the target corrosion level of 20%.

Before the corrosion process was started, one end of the rebar was insulated to ensure that only the bonded zone was corroded. And the lower part of the rebar (immerged in 5%NaCl solution) was wrapped with insulated plastic tape and, moreover, coated with paraffin.

2.4 Loading and measuring instrumentation

An MTS300 was used for the loading test, and a specially designed and fabricated loading frame was designed for the tested specimens. Fig. 4(a) shows the schematic drawing of the loading system and Fig. 4(b)

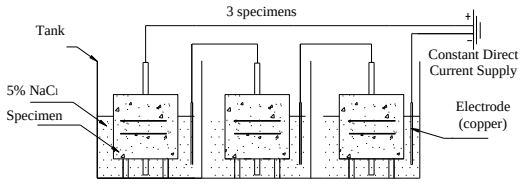

(a) Schematic drawing

(b) Photograph

Fig. 3 Schematic representation of the electrochemical system

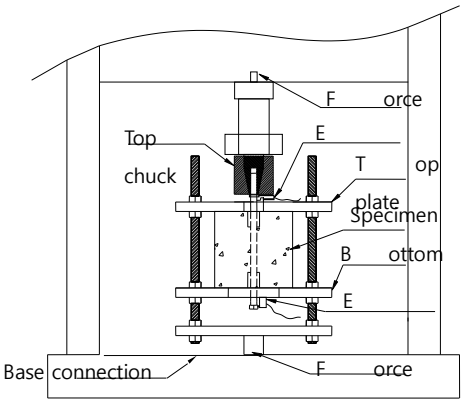

(a) Schematic drawing

(b) MTS300 with tested specimen

Fig. 4 Loading and measuring system

Fig. 5 Rebars at different corrosion levels from left to right: 0.13%, 3.45%, 6.87%, 9.55%, 14.60%

shows the photo. In order to eliminate the effects of friction force between the concrete and the steel plate surfaces, butter was applied to the surface of concrete for lubrication. Meanwhile, two extensometers with precision of ±0.001 mm was applied to measure the loading-end and the free-end slips. The loading-end slip was limited to 3mm due to space limitations. The experiment consisted of two force sensors, and the lower force sensor was installed on the MTS 300 so that the force and slip data could be collected at the same time. A Donghua SN3816 data logger was used to collect the lower force sensor and the two extensometers' data. There were three different loading schemes in this study. The first was monotonic loading until pull-out. The second was ±0.1mm cyclic free-end slip loading run 10 cycles followed by pull-out. The third consisted first of ±5kN loading for 3 cycles, then ±0.1mm~±0.3mm~±0.6 mm free-end slip loading, each amplitude loading for 3 cycles, followed by pull-out.

3. Test results

After the loading test, the corroded rebar was derived. The corroded rebar was soaked in diluted hydrochloric acid for approximately 30min, and then the rust was washed away. The steel was later submerged in saturated $Ca(OH)_2$ solution to remove the hydrochloric-acid. Then it was dried and weighed to get the actual mass loss calculated by the following formula

$$\xi_s = \frac{m_0 - m_t}{m_0} \times 100\% \quad (2)$$

where ξ_s is the mass loss, m_0 is mass of rebar before corrosion, and m_t is the mass of rebar after removal of the corrosion products.

Fig. 5 shows the five corroded rebars at five different actual levels of corrosion. It was observed that the mass loss of rebar was relatively uniform along the bonded section at lower levels of corrosion (<10%). Damage at higher levels of corrosion became more serious than that of lower corrosion levels. Fig. 5 shows that the rib of rebar was almost corroded away for the 14.6% corrosion level.

3.1 Bond-slip curves

3.1.1 Monotonic pull-out loading

Fig. 6 shows five typical bond stress vs. free-end slip curves. The bond stress was derived according to the measured load force by the following equation

$$\tau = \frac{P}{\pi d l} \quad (3)$$

where l is the bond length, d is the diameter of rebar, and P is the measured pullout load force. In this paper, it is found that the loaded end slip was slightly larger than that of free-end slip when bond stress was the same. The bond stress vs. free-end slip curves are very similar to bond stress vs. loaded end slip curves, and only the free-end slip values

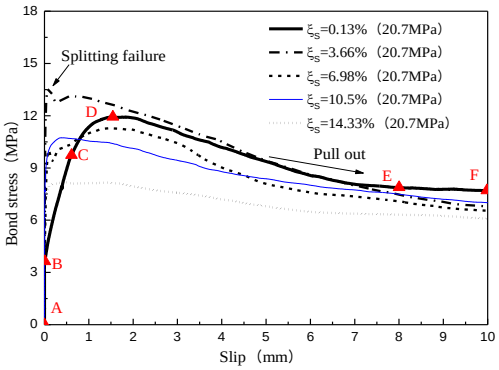

(a) Bond stress-slip curve (20.7 MPa)

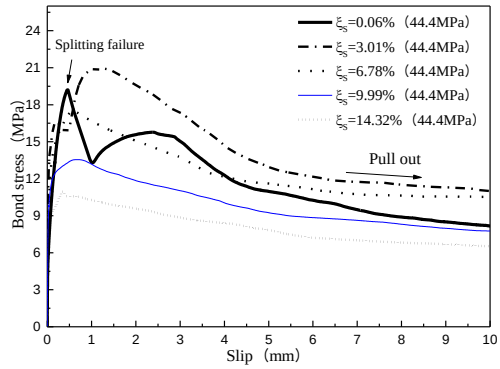

(b) Bond stress-slip curve (44.4 MPa)

Fig. 6 Bond stress-slip curves under monotonic pull-out loading

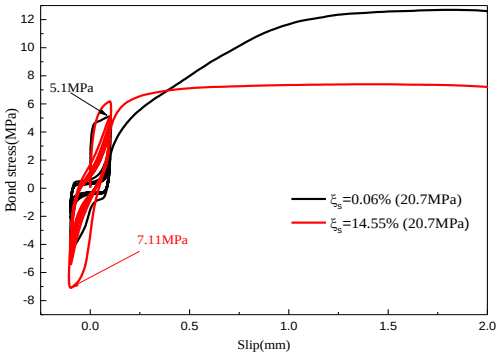

(a) Bond stress-slip curve 20.7 MPa

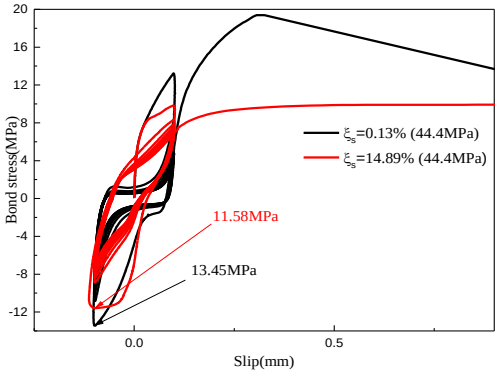

(b) Bond stress-slip curve 44.4 MPa

Fig. 7 Bond stress-slip curves under ±0.1 mm slip followed by pull out

were used in the following analysis, as most other reported studies have used the free-end slip.

The effects of rebar corrosion were obvious in Fig. 6. Fig. 6(a) shows the bond-slip curves for the concrete strength of 20.7 MPa. It can be observed that there were five stages for the curves of intact specimens and specimens with 10.5% corrosion level (Xu 1994). The bond stress increased very fast at the first stage (micro-slip stage, A-B), the tangent stiffness of curve was much larger than that of the following stages, and the slip value corresponding to this stage was very small. In the second stage (slip stage, B-C), the bond-slip curve showed a tendency as the bond stress increased gradually with an increasing slip value, until it reached to a turning point. For the third stage (splitting stage, C-D), the bond stress increased slowly before reaching the bond strength (maximum bond stress), which corresponded to bond failure (Wu and Zhao 2013). The curve showed a fourth stage (decline stage, D-E) where the bond stress decreased continuously after the bond strength until the slip value reached to about 8.0mm. Then the bond-slip curves became shallower and reached to the residual bond stress corresponding to 10mm free-end slip (residual stage, E-F). The curve of specimen with 0.13% corrosion level actually shows the pull-out bond failure mode as previously described. And the curve of specimen with 14.33% corrosion level also shows the pull-out failure mode; however, the five stages of the curve are not obvious compared with the specimens with 0.13% and 10.15% corrosion level. The reason behind this phenomenon was due to ribs were almost corroded away for rebar with high corrosion level, so the mechanical inter-action force between ribs and concrete was greatly reduced, and the pull-out curve is similar to that of plain bar in concrete (Kivell 2012).

For the specimens with the 3.66% and 6.98% corrosion levels, the bond-slip curves shows splitting failure mode. The slopes of the first two stages are much larger than that for intact specimens. Then the curves reaches a peak, which indicates the splitting failure. For the curve of 3.66% corrosion level, the peak also indicated the bond strength. However, for the curve of 6.98% corrosion level, bond stress just dropped suddenly and then continued increasing up to the maximum bond stress. Compared with the un-corroded specimens, the value of free-end slip corresponding to the peak was much smaller, only about 0.1mm. For the curve of the specimen with 3.66% corrosion level, the bond strength was obviously larger than that of the intact specimen. However, the free-end slip corresponding to bond strength was only about 0.15mm, which was much smaller than that of the intact specimen. Then the bond stress dropped down and was almost the same with that of specimen with un-corroded rebar. It could also be clearly observed that the higher the corrosion level, the lower the bond strength for the specimens with corrosion levels higher than 6.98%.

3.1.2 Cyclic slip loading followed by pull out

Fig. 7 shows the bond stress-slip curves of specimens with two different kinds of concrete mixes under ±0.1 mm slip loading followed by pull-out. The bond stress–slip

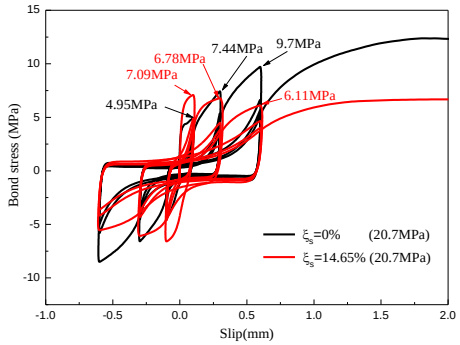

(a) Bond stress-slip curve (20.7MPa)

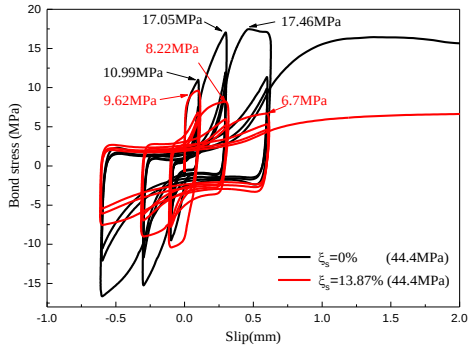

(b) Bond stress-slip curve (44.4MPa)

Fig. 8 Bond stress-slip curves under ±5 kN~±0.1 mm~±0.3 mm~±0.6 mm followed by pull out

curve started at a slip value close to zero, and then increased to a local peak value of the bond stress. After the first cyclic loading and reversed loading, the local bond stress peak decreased rapidly. For the C20 specimens, the maximum bond stress of specimens with 14.55% corrosion level was smaller than that of intact specimens. And the local maximum bond stress for the 1st cycle was about 44.57% higher than that for the 2nd cycle. For the C40 specimens, the maximum bond stress had the same trend compared with that of C20 specimens. It clearly shows that the closed loops are spindle shaped for the corroded specimens, while they are "S" shaped for the intact specimens. It could be confirmed that the corrosion would increase the cyclic loading performance of corroded specimens at this tiny loading level. It is interesting that for the C20 specimens, the maximum bond stress in cyclic phase of specimens with 14.55%, 14.78%, 13.45% and 14.21% corrosion level was larger than that of intact specimens. For the C40 specimens, the maximum bond stress in cyclic phase of specimens with 13.92% and 15.44% corrosion level was smaller than that of intact specimens. However, for C40 specimen with 14.89% corrosion level, the maximum bond tress in cyclic phase was larger than that of intact specimens. This phenomenon might suggest that the corrosion degradation of C40 specimens was more serious than that of C20 specimens.

Fig. 8 shows the tested bond stress-slip curves of specimens with two different kinds of concrete mixes under ±5 kN~ ±0.1 mm~ ±0.3 mm~ ±0.6 mm cyclic slip loading followed by pull-out. Considering that the stress-slip curve was almost linear during the first 3 cyclic loading processes, the first 3 cycles of ±5 kN loading could not be observed

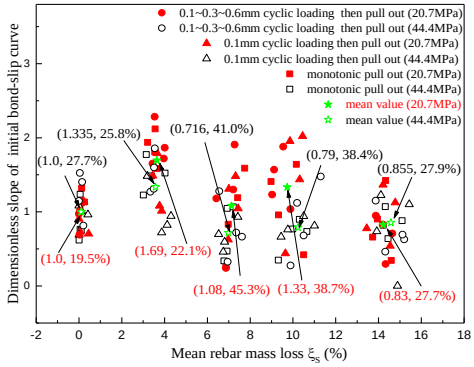

Fig. 9 Dimensionless slope of initial bond-slip curve vs. mean rebar mass loss

clearly. This just confirmed that there was little damage during first three cyclic loadings. For the C20 specimens at the 14.65% corrosion level, the bond strength and the corresponding slip value decreased drastically compared with those of the intact specimens. For the C40 specimens at the 13.87% corrosion level, the bond strength and the corresponding slip value had same trend with the C20 specimens at the 14.65% corrosion level.

It can be seen that for the intact C40 specimens, the maximum bond stress appeared in the 10th cycle of the bond slip curve; but for the intact C20 specimens, the maximum bond stress appeared after the 10th cycle. However, for the C40 specimen with 13.87% corrosion level and the C20 specimen with 14.65% corrosion level, the maximum bond stress appeared in the 4th cycle of the bond-slip curves. It could be concluded that corrosion significantly increased the brittleness of C20 and C40 specimens, especially for C20 specimens.

3.2 Slope of initial bond-slip curve

Fig. 9 shows the dimensionless slope of the initial bond-slip curve for all of tested specimens. The dimensionless slope of the initial bond-slip curve was defined as the slope of the initial bond-slip curve divided by mean value of the slope of the initial bond-slip curve of the intact specimens. And the following parameters are also nondimensionalized based on the above method. The circular symbols indicate the cases of varied amplitude cyclic loading, the triangular symbols indicate the cases of constant amplitude cyclic loading, the square symbols indicate the case of monotonic loading, and the pentagram indicates the mean value in Fig. 9. The mean value and the coefficient of variation (Everitt 1998) are both shown near the pentagram in a bracket and separated by a comma, respectively. The above rule is also applied to the following figures. The slope of the initial bond-slip curve was defined as the slope of tangent line which was the best linear fitting of the bond-slip curve data with loading force from 0-10 kN (bond stress from 0 to 2.21 MPa). Compared with the specimens with un-corroded rebar, the mean dimensionless slope of the initial bond-slip curve of the C20 specimens was increased 69.5% for the 3.64% rebar corrosion level; but the increment was only 33.5% for the C40 specimens. The mean dimensionless

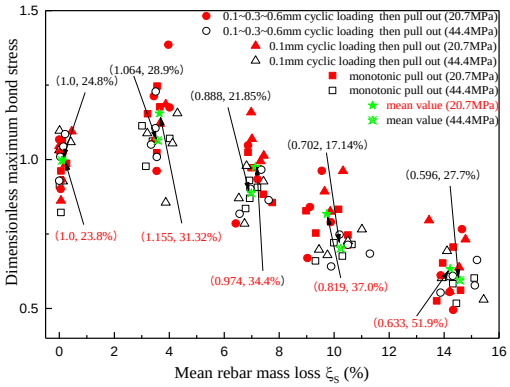

Fig. 10 Dimensionless bond strength vs. mean rebar mass loss

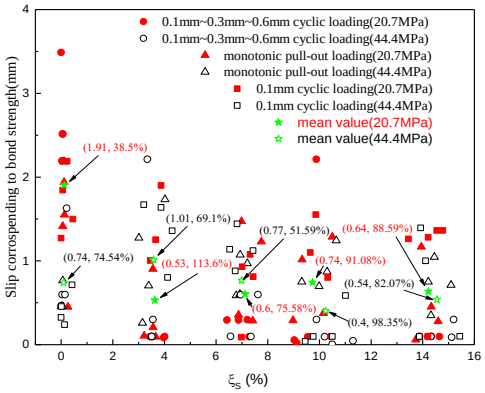

Fig. 11 Slip value corresponding to maximum bond stress

slope of the initial bond-slip curve decreased as the rebar corrosion level continued increasing. It can be concluded that the slope increment of the C20 specimens was larger than that of C40 specimens at the lower corrosion level. Moreover, for the C20 corroded specimens with 3.6%, 7.1% and 9.7% corrosion levels, the mean slope of initial bond-slip value was larger than that for intact specimens. For the C40 corroded specimens, the mean slope of the initial bond-slip curve was smaller than that for intact specimens, except for the slope of the initial bond-slip curve of specimen with 3.58% corrosion level. All in all, the coefficient of variation of corroded specimens was obviously larger than that of specimens with intact rebar.

3.3 Bond strength

Fig. 10 shows the dimensionless bond strength vs. mean rebar mass loss. It clearly shows that the coefficient of variation for most of the corroded specimens was larger than that for intact specimens. It also shows that slight corrosion enhanced the bond strength. The C20 specimens had an increment of 15.5% in the bond strength for the 3.6% corrosion level compared to that of intact rebar. While for C40 specimens, the increment was only 6.4%. Following the 3.6% corrosion level, a decreasing trend for the mean bond strength could be observed for higher steel corrosion levels; the decrement of the C20 specimens was recorded as 36.7% for 14.22% rebar corrosion level. The decrement of the C40 specimens was recorded as 40.4% for a 14.58% rebar corrosion level. This just proved that the concrete mix had obvious effects on the bond strength degradation. It can be concluded that the higher concrete strength, the higher percentage of bond strength degradation due to steel corrosion. This just proved the results of Yalciner *et al*. (2012).

3.4 Slip value corresponding to maximum bond stress

Fig. 11 shows the slip value corresponding to bond strength vs. the reinforcement corrosion level. It clearly shows that the rebar corrosion level and the concrete mix had effects on the slip value.

For the C20 specimens, the slip value corresponding to

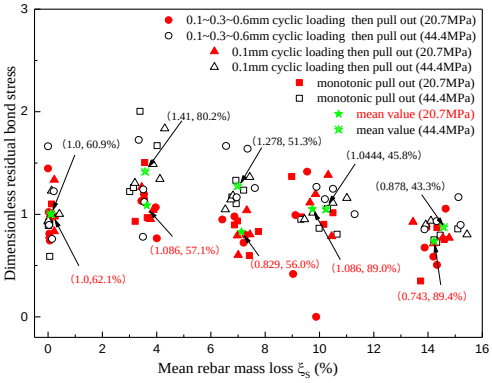

Fig. 12 Dimensionless residual bond stress vs. mean rebar mass loss

the bond strength of corroded specimens was smaller than that of intact specimens. However, for the C40 specimens, the slip values of specimens with 3.58% and 6.99% corrosion levels was larger than that of intact specimens. Then, as the continued increasing of corrosion level, the slip value was smaller than that of intact specimens. Overall, Fig. 11 shows the trend that the slip value decreased with increasing corrosion level. And the decrement of slip of the C20 specimens was larger than that of C40 specimens. For example, the decrement of slip value of C20 specimens was up to 78.5% for a 14.22% rebar corrosion level, but the decrement of C40 specimens was only 27.2% for 14.55% rebar corrosion level. The coefficient of variation was very large, the reason was due to the two different kinds of failure mode (pull-out and splitting) are co-existing in the specimens.

3.5 Residual bond stress

Fig. 12 shows the dimensionless residual bond stress corresponding to 10 mm free-end slip. The residual bond stress was the friction between steel and concrete after 10 mm free-end slip loading damage. It clearly shows that the slight corrosion might increase the mean residual bond stress. For example, the C20 specimens with 3.6% corrosion level increased 8.6% compared to intact specimens, and the C40 specimens with 3.58% corrosion level increased 41% compared to the intact specimens. For the C40 specimens with higher corrosion levels (>6.99%),

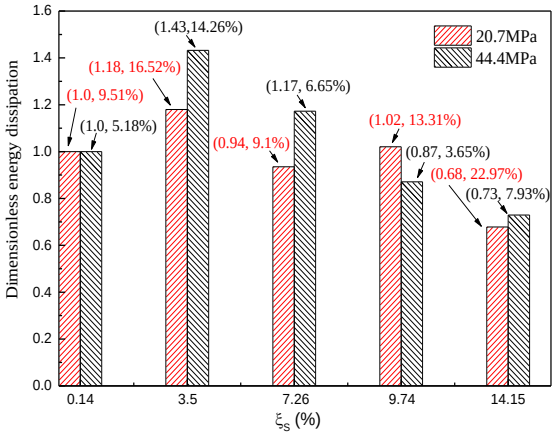

Fig. 13 Dimensionless energy dissipation vs. mean rebar mass loss

the mean residual bond stress decreased gradually as the corrosion level increased. However, for the C20 specimens with 3.64% and 9.74% corrosion level, the mean residual bond stress was the maximum, and the mean residual bond stress was larger than that of specimen with intact rebar. As a whole, the C20 specimens also shows a trend that the residual bond stress decreased with increase of corrosion level. Moreover, the C40 specimens shows a relative higher dimensionless residual bond stress compared to that of the C20 specimens for the different corrosion levels.

3.6 Energy dissipation

3.6.1 Monotonic pull-out loading

Fig. 13 shows the dimensionless energy dissipation for monotonic pull-out loading. The energy dissipation here was defined as integral area of the bond-force-slip curves with the slip value from 0 to 10 mm. For the 3.55% rebar corrosion level, the energy dissipation of specimens (C20 and C40) increased slightly compared to intact specimens. However, for higher rebar corrosion levels, a diminishing of energy dissipation could be observed for all specimens. It was also seen that the energy dissipation of 14.15% corrosion level was reduced to be 68% of that of intact rebar for the specimens with 20.7 MPa concrete strength, while for the specimens with 44.4 MPa concrete strength, the number is 73%. Besides this, Fig. 13 also shows a trend of increased coefficient of variation for corroded members compared to that of un-corroded specimens.

3.6.2 Cyclic slip loading

The energy dissipation in one cycle was derived by calculating the area of the hysteresis loop in the bond-slip curves. Fig. 14 shows the dimensionless energy dissipation of each cycle under ±0.1 mm cyclic loading. It shows that all the corroded specimens displayed an increased energy dissipation as compared to the intact specimens. For the C20 specimens, the mean energy dissipation of the 14.67% corrosion level was increased by 149% compared to that of intact specimens, while the C40 specimens only increased 17% at the same corrosion level. In this way, the effects of different concrete mixes on the mean energy dissipation

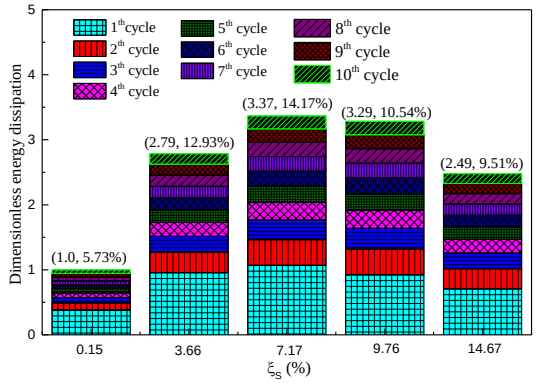

(a) 20.7MPa

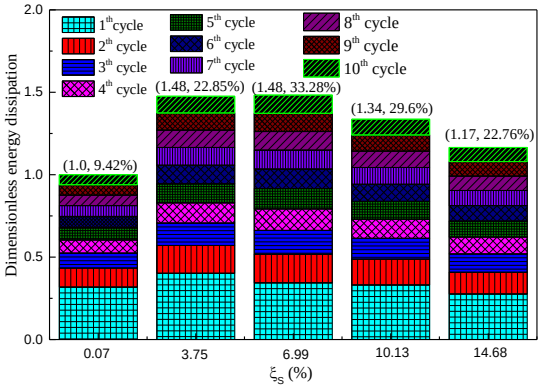

(b) 44.4MPa

Fig. 14 Dimensionless energy dissipation vs. mean rebar mass loss

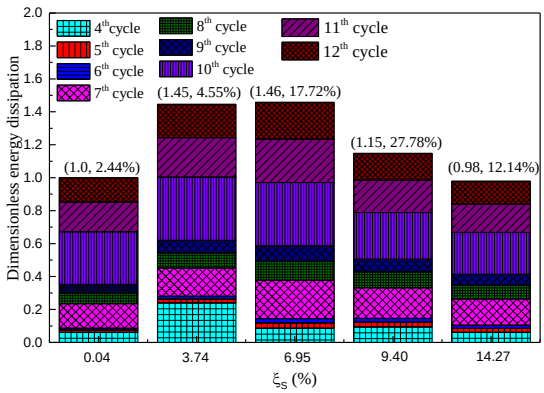

(a) 20.7MPa

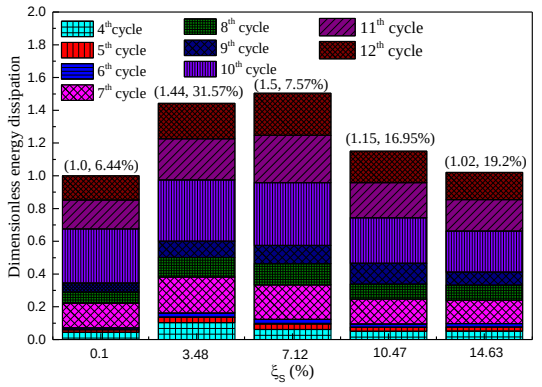

(b) 44.4MPa

Fig. 15 Dimensionless energy dissipation vs. mean rebar mass loss

cannot be ignored. For the C20 specimens, the mean energy dissipation at the 7.1% corrosion level was the maximum, and the maximum mean energy dissipation was increased by 237% compared to that of intact specimens. But for the C40 specimens, the energy dissipation at the 3.58% and 6.99% corrosion levels were the largest, and the maximum mean energy dissipation was only increased by 48% compared to that of intact specimens.

Fig. 15 shows the dimensionless energy dissipation of cyclic stage under ±5kN~±0.1 mm~±0.3 mm~±0.6 mm cyclic loading. Considering that the bond-slip curve of the first three cycles was almost linear during the loading and unloading processes, the energy dissipation of the first three cycles are not calculated. For the C20 specimens, the mean dimensionless total energy dissipation increased with the increasing of corrosion level when the corrosion level was lower than 6.95%. The energy dissipation of specimen with 6.95% corrosion level was the maximum and the maximum value was increased by 46% compared with that of intact specimens. As the rebar corrosion level continued increasing, the mean dimensionless total energy dissipation decreased. The mean energy dissipation of the C40 specimens is similar to that of the C20 specimens. However, the maximum value of C40 specimens was increased by 50% compared with that of intact specimens. As a whole, it also shows an increased coefficient of variation for corroded members as compared with un-corroded members.

3.7 Frictional bond resistance

Fig. 16 shows the dimensionless frictional bond resistance of the last three cycles (10^{th}~12^{th}) under ±5 kN~±0.1 mm~±0.3 mm~±0.6 mm cyclic loading. The frictional bond resistance was defined by the following equation (Zhou *et al.* 2015b)

$$\tau_f = \frac{\tau_{f,min}+\tau_{f,max}}{2} \quad (4)$$

where τ_f is the frictional bond resistance, $\tau_{f,\min}$ is the minimum value in the forward direction, $\tau_{f,\max}$ is the absolute value of maximum value in the negative direction.

The dimensionless frictional bond resistance was defined as the frictional bond resistance divided by frictional bond resistance of 12^{th} cycle of intact specimen. Fig. 16(a) shows that the dimensionless frictional bond resistance of C20 specimens decreased with the increasing of cycle number. The decrement of the dimensionless frictional bond resistance of corroded specimens was larger than that of the intact specimens. For specimens with lower corrosion levels, the frictional bond resistance increased with the increase of corrosion level, but then decreased with continued increase of corrosion level. And the dimensionless frictional bond resistance reached to the maximum value at the 7.13% corrosion level. Fig. 16(b) shows that the dimensionless frictional bond resistance of C40 specimens decreased with the increasing of cycle number. Also, it shows the same trend with the 20.7 MPa specimens, the maximum dimensionless frictional bond resistance appeared at the 6.99% corrosion level. For the C40 specimens, the increment of the dimensionless frictional bond resistance was larger than that of the C20 specimens before reaching to the maximum value; but the decrement of the dimensionless frictional bond resistance was smaller than that of C20 specimens after the maximum value. More interesting, Fig. 16 clearly shows an increment of frictional bond resistance for all of the corroded specimens compared to the intact specimens.

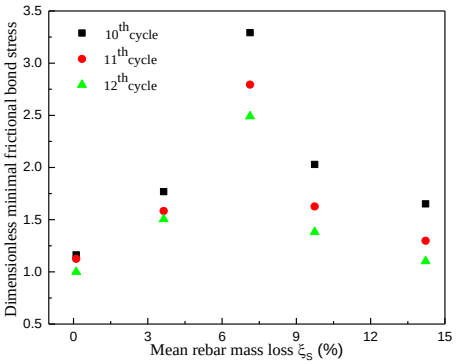

(a) 20.7MPa

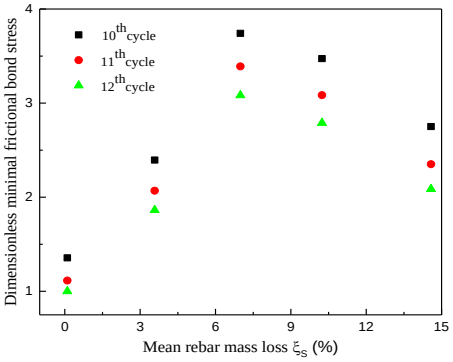

(b) 44.4 MPa

Fig. 16 Dimensionless frictional bond resistance vs. mean rebar mass loss

4. Further discussion

Bond stress is mainly composed of three parts: chemical adhesion, mechanical interaction between rib and concrete and frictional resistance. Due to the fact that bond strength happened with an obvious slip between rebar and concrete, it was supposed that the chemical adhesion was destroyed when bond stress reached the maximum (bond strength). So in the following, it was assumed that the mechanical interaction stress could be derived by deducting the frictional resistance from the bond strength.

Fig. 17 shows the dimensionless mechanical interaction stress of all tested specimens. It is clearly indicating that the C20 specimens show an increment in mechanical interaction stress for a 3.6% corrosion level compared to that of intact specimens. As corrosion level increased, the mean mechanical interaction stress of C20 specimens decreased gradually, and the mean mechanical interaction stress of 14.22% steel corrosion level decreased by 53.2% compared to that of intact specimens. The mean mechanical interaction stress of the specimens C40 always decreased, and the mean mechanical interaction stress of 14.58%

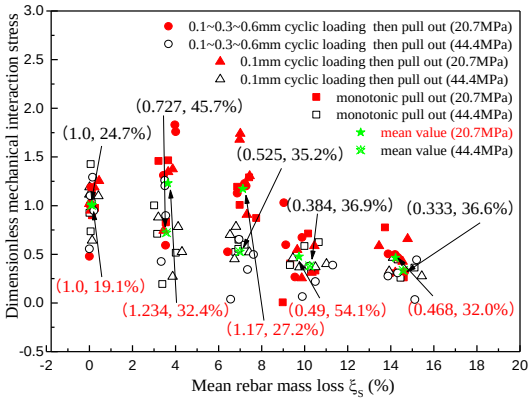

Fig. 17 Mechanical interaction stress vs. mean rebar mass loss

corrosion level decreased by 66.67% compared to that of intact specimens. Moreover, the coefficient of variation of corroded specimens was also larger than that of specimens with intact rebar.

5. Conclusions

This paper reports a detailed experimental study of steel corrosion effects on bond performance of reinforcing steel in two different concrete mixes. Monotonic pullout loading tests, constant and varied amplitude cyclic loading tests of 120 specimens were carried out.

- The results of this test shows that slight rebar corrosion may increase slope of the initial bond-slip curve, the bond strength, the residual bond stress, the frictional bond resistance and the energy dissipation for C20 and C40 specimens. For C20 and C40 specimens with higher corrosion level, in general, the slope of initial bond-slip curve, bond strength, the residual bond stress, the frictional bond resistance and the energy dissipation show a trend that all of them decreased with the continued increase of corrosion level.
- For the C20 specimens with slight corrosion level (<3.66% corrosion level), the increment of the slope of the initial bond-slip curve was larger than that of C40 specimens. For the frictional bond resistance, the increment of C20 specimens with lower corrosion level (<6.99% corrosion level) was smaller than that of C40 specimens. The dimensionless energy dissipation of C20 specimens was obviously larger than that of C40 for the ±0.1mm cyclic loading condition; however, they were almost the same for the varied cyclic slip loading condition. The mechanical interaction stress of the C20 specimens shows an increment at lower corrosion levels, but at higher corrosion levels, it decreased with the increase in corrosion level. However, the mechanical interaction stress of the C40 specimens always decreased with the increase in corrosion level.
- In general, the coefficients of variation of the bond-slip parameters of corroded specimens are larger than that of intact specimens; the maximum increment is about 200%. The coefficients of variation of the test parameters are large and further investigation about the mechanism behind this phenomenon is needed.

This study shows the effects of reinforcement corrosion and different concrete mixes on the bond performance between reinforcement and concrete. It was confirmed that there were obvious difference between the test results of the two concrete mix. It was also found that the coefficient of variation of bond parameters of corroded members were obviously larger than that of un-corroded members. More detail investigation and verification are still urgently needed to further develop a stochastic bond-slip model to quantify these effects in the near future.

Acknowledgements

The work described in this paper was financially supported by the National Natural Science Foundation of China (Grant No. 51378313) and the Ministry of Science and Technology for the 973-project (No. 2011CB013604), to whom the writers are grateful.

References

Almusallam, A.A., Al-Gahtani, A.S. and Aziz, A.R (1996), "Effect of steel corrosion on bond strength", *Constr. Build. Mater.*, **10**(2), 123-129.

Bhargava, K., Ghosh, A., Mori, Y. and Ramanjam, S. (2008), "Suggested empirical models for corrosion-Induced bond degradation in reinforced concrete", *ASCE J. Struct. Eng.*, **134**, 221-230.

Chen, H.P. and Nepal, J. (2015), "Stochastic modelling and lifecycle performance assessment of bond strength of corroded reinforcement in concrete", *Struct. Eng. Mech.*, **54**(2), 319-336.

Coronelli, D., Hanjari, K.Z. and Lundgren, K. (2013), "Severely corroded RC with Cover Cracking", *J. Struct. Eng.*, **139**(139), 221-232.

Eligehausen, R., Popov, E.P. and Bertero, V.V. (1983), "Local bond stress-slip relationships of deformed bars under generalized excitations", EERC Report No. UCB/EERC-83/23, University of California at Berkeley, California.

Everitt, B.S. (1998), *The Cambridge Dictionary of Statistics*, Cambridge University Press, Cambridge, UK, New York.

Fang, C.Q., Gylltoft, K., Lundgren, K. and Plos, M. (2006), "Effect of corrosion on bond in reinforced concrete under cyclic loading", *Cement Concrete Res.*, **36**(3), 548-555.

Fang, C.Q., Lundgren, K., Chen, L. and Zhu, C. (2004), "Corrosion influence on bond in reinforced concrete", *Cement Concrete Res.*, **34**(11), 2159-2167.

Kivell, A. (2012), "Effects of bond deterioration due to corrosion on seismic performance of reinforced concrete structures", Thesis of University of Canterbury of New Zealand.

Kivell, A., Palermo, A. and Scott A. (2015),"Complete model of corrosion-degraded cyclic bond performance in reinforced concrete", *J. Struct. Eng.*, **141**(9), 04014222.

Mangat, P.S. and Elgarf, M.S. (1999), "Bond characteristics of corroding steel in concrete beams", *Mater. Struct.*, **32**, 89-97.

Sæther, I. (2011), "Bond deterioration of corroded steel bars in concrete", *Struct. Eng. Mech.*, **7**(6), 415-429.

Serhat, D. and Metin, H. (2015), "Investigation of bond-slip modeling methods used in FE analysis of RC members", *Struct. Eng. Mech.*, **56**(2), 275-291.

Shetty, A., Venkataramana, K. and Narayan K.S. B. (2014),

"Flexural bond strength behaviour in OPC concrete of NBS beam for various corrosion levels", *Struct. Eng. Mech.*, **49**(1), 81-93.

Wu, Y.F. and Zhao, X.M. (2013), "Unified bond stress-slip model for reinforced concrete", *ASCE J. Struct. Eng.*, **139**(11), 1951-1962.

Xu, Y.L, Shen, W.D. and Wang, H. (1994), "An experimental study of bond anchorage properties of bars in concrete", *J. Build. Struct.*, **3**, 26-37.

Yalciner, H., Eren, O. and Sensoy, S. (2012), "An experimental study on the bond strength between rebars and concrete as a function of concrete cover, strength and corrosion level", *Cement Concrete Res.*, **42**(5), 643-655.

Zhao, Y.X., Lin, H.W., Wu, K. and Jin, W.L. (2013), "Bond behaviour of normal/recycled concrete and corroded steel bars", *Constr. Build. Mater.*., **4**8, 348-359.

Zhou, H.J., Lu, J.L., Xv, X., Zhou, Y.W. and Xing F. (2015a), "Experimental study of bond-slip performance of corroded reinforced concrete under cyclic loading", *Adv. Mech. Eng.*, **7**(3), 1687814015573787.

Zhou, H.J., Xv, X., Dong, B.Q. and Xing, F. (2015b), "Effects of stirrup corrosion on bond-slip performance of reinforcing steel in concrete: An experimental study", *Constr. Build. Mater.*, **93**, 257-266.